Zn Bath Corrosion Behavior of the Martensitic Stainless Steels (1.4095-Type) After Variation of the Si and Cr Content in Comparison to the Ferrite-Free 316L Type (1.4409.01)

The martensitic cast steel 1.4095 shows a good corrosion resistance in liquid Zn-bath in a temperature range up to T = 480°C. In this study, the chemical composition of the 1.4095 material has been modified with respect to Si and Cr content. These modified alloys will be subjected to a static liquid corrosion test in a Zn-bath for different test durations and test temperatures. Additionally, the mechanical properties will be presented. The results are compared with the corrosion results of the ferrite-free modified 316L. Afterwards the tested samples are evaluated by means of mass loss, optical microscopy and scanning electron microscopy.

Authors

Tobias Simon (pictured), Kuhn Special Steel, Radevormwald, Germany
t.simon@kuhn-edelstahl.com

Frank Wischnowski, Kuhn Special Steel, Radevormwald, Germany

Introduction

In 2022, there were 87 continuous hot-dip coating lines operating in North America.[1] Most of the continuous galvanizing lines are capable of galvanizing and galvannealing.[1] Furthermore, as of the time of this writing, there are nine new continuous galvanizing lines publicly announced to be built.[1] This reflects the growing demand for hot-dip galvanized sheet.[2] The worldwide demand for zinc (Zn) is assumed to grow at a rate of 0.9–1.9% in the years 2024–2026.[2] The worldwide usage of zinc can be correlated to the production of galvanized steel sheet.[3] The capacity and requirements of new continuous galvanizing lines leads to new challenges for the complete process and the materials used within the continuous galvanizing process. One essential part of the process with respect to corrosion and mechanical loads is the pot equipment, specifically sink rolls, stabilizing rolls, bearings and the surrounding constructions. These parts are continuously subjected to a corrosive environment and mechanical and wear loads, which lead to a relatively short lifetime. For the Zn bath equipment such as stabilizing rolls and sink rolls, which are essential components for continuous galvanizing lines, the requirements with respect to surface quality, service lifetime and mechanical strength are also increasing. In this empirical study, different martensitic-ferritic and austenitic materials were exposed to a liquid Zn bath in a static corrosion test. The materials were all centrifugal cast alloys. After these static corrosion tests, the samples were extracted out of the test rig and evaluated with respect to the grown layers, reduction in diameter and microstructure. Additionally, the mechanical properties were investigated at room temperature and at an elevated temperature of T = 480°C.

Experimental Methods and Materials

In this empirical study, materials used for sink and stabilizing rolls and new experimental alloys are subjected to a static liquid Zn bath corrosion test. A Zn bath with about 99.0% Zn and 1% Al was used. The chemical analysis of the zinc bath was measured after every corrosion test to check for changes in chemical analysis between different tests. Table 1 summarizes the chemical analysis of the used Zn bath before and after the static corrosion test.

Table 1

Optical Emission Spectroscopy Analysis of the Used Zn Bath Prior and After the Static Corrosion Test at T = 480°C

No.	Date	Al	Cu	Fe	Pb	Sn	Zn	Notes
1	4 December 2023	1.1900	0.0023	0.2400	0.0049	0.0097	Balance	Prior to the corrosion test at T = 480°C
2	3 January 2024	0.4250	0.0014	0.0600	0.0043	0.0060	Balance	After the corrosion test at T = 480°C
3	4 January 2024	0.5220	0.0016	0.1100	0.0042	0.0079	Balance	Added Zn + Al prior to the test at T = 500°C

Figure 1

The drawing of the test sample is shown on the left side. In the middle a live test can be seen — white arrows are showing on the top of the samples. On the right side, the test rig for the corrosion experiments in the heat treatment furnace is shown prior to a test.

Table 1 shows the chemical analysis of the used Zn bath prior to and after the corrosion test. The chemical composition was measured via optical emission spectroscopy (OES). It can be clearly seen that there is a Zn-based bath with approximately 1% Al content.

The static corrosion test in the liquid Zn bath was performed in a self-constructed test rig consisting of a crucible in an electric-heated furnace. For these tests, a sample holder exists which can take up to 10 different samples at the same time for the static corrosion test. This has the advantage that 10 samples can be exposed to the corrosive bath at the same time and a high throughput with respect to the number of alloys/batches tested is possible. This experimental setup is flexible with respect to test duration and test temperature.

Fig. 1 also shows a drawing of the sample geometry used and the setup of the test rig. The crucible shown in the middle and right pictures contains the liquid Zn bath and the corrosion samples are statically immersed in the Zn bath for the duration of the test at the designated test temperature. The parameters for the corrosion tests in this study can be found in Table 2. In the first experiment, a long-term static corrosion test was conducted for 715 hours (~30 days) at a temperature of T = 480°C. The second test was conducted at a temperature of T = 500°C but the test was canceled only after a test period of only 100 hours due to a failure of the test rig. More details of the rig failure will be discussed later.

Seven different materials with different chemical analyses were tested in this study. The details of the chemical analysis can be seen in Table 3. Three materials act as

Table 2

Test Parameters for the Static Corrosion Tests in the Liquid Zn Bath

Corrosion media	Zn +1% Al (analysis in Table 1)	
Temperatures	480°C	500°C
Corrosion time	715 hours	100 hours*

*This experiment was stopped prior to the planned end of test because of a failure of the test rig. See the experimental results for more details.

references. First the ferrite-free, austenitic 316L material was chosen. Additionally, the martensitic-ferritic stainless steel 1.4095 and 1.4096 material was selected. The four other tested alloys were modified ~1.4095 alloy types with a variation of the Cr and Si content. The tested Cr range was from 4.0% up to 10.0% and the tested Si contents varied from 1.5% up to 3.0% for the martensitic-ferritic stainless steel. This is illustrated by the bolded analysis of Cr and Si in Table 3.

The tensile tests on the seven different materials were performed in a heat-treated condition. The ferrite-free 316L material was solution-annealed at T = 1,080°C and quenched in water. The martensitic-ferritic alloys were hardened at T = 1,040°C and quenched in air. The subsequent annealing took place at a temperature of T = 600°C for all samples. Afterwards, round tensile test specimens with a diameter of 10 mm were machined and tensile tested at T = 20°C and at T = 480°C.

After the corrosion tests, all samples were examined using optical microscopy. Selected alloys were also examined using scanning electron microscopy (SEM) combined with energy-dispersive x-ray (EDX) chemical analysis to gain an understanding of the different phases created during the corrosion testing. Additionally, the dimensions of the test pieces were evaluated after testing for an empirical comparison and to evaluate if the materials were promising with respect to their application in continuous hot-dip galvanizing lines.

Results: Mechanical Testing — Tensile Test

The tested materials were mechanically tested prior to the corrosion test. The martensitic-ferritic stainless steels based on the 1.4095 material were all heat treated in the same way in a laboratory heat treatment furnace. The samples were hardened at T = 1,040°C for 3 hours and then quenched in air. The annealing of the materials took place at 600°C for 3 hours followed by a cooling

Table 3

The Seven Different Materials Tested in the Static Corrosion Tests in the Liquid Zn Bath and the Corresponding Chemical Analysis Determined Using Optical Emission Spectroscopy (OES). All elements are shown in wt. %. The bolded elements are illustrating the variated chemical elements of Cr and Si.

Mat. No.	Comments	C	Si	Mn	P	S	Cr	Mo	Ni	Fe
1.4095	1.4095	0.0955	**1.5000**	0.8340	0.0156	0.0048	**10.1900**	0.0666	0.2600	Balance
1.4096		0.1220	**2.2900**	0.4770	0.0142	0.0054	**7.9800**	0.0644	1.1300	Balance
~1.4095	3%Si, 6%Cr	0.1100	**2.9400**	0.4610	0.0086	0.0059	**6.0900**	0.0114	0.1500	Balance
~1.4095	3%Si, 4%Cr	0.1240	**2.9700**	0.4900	0.0092	0.0065	**4.2800**	0.0126	0.1500	Balance
~1.4095	2.5%Si, 4%Cr	0.1020	**2.3700**	0.4600	0.0072	0.0051	**4.1900**	0.0119	0.1400	Balance
~1.4095	2%Si, 4%Cr	0.1130	**2.0600**	0.5150	0.0086	0.0060	**4.1200**	0.0118	0.1000	Balance
1.4409.01	316L ferrite free	0.0265	0.4600	1.7900	0.0268	0.0056	18.4000	2.0800	12.0100	Balance

Figure 2

Summary of the results of the tensile tests of the tested martensitic-ferritic and austenitic alloys. On the left side the yield strength and the ultimate tensile strength is shown (values in MPa/N/mm^2), while on the right side the elongation at fracture is presented in %. The test temperature was for this series T = 20°C.

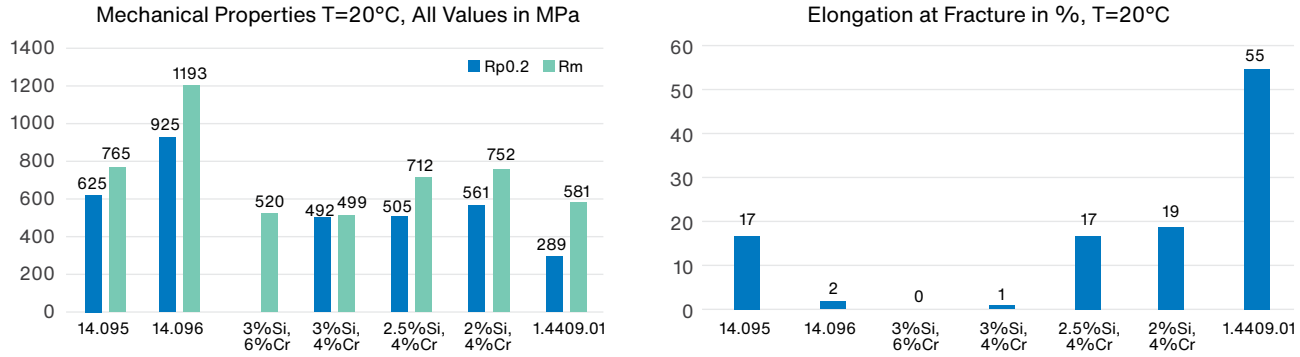

on air. The austenitic stainless steel 1.4409.01 was solution annealed at a temperature of T = 1,080°C and then quenched in water. After this heat treatment, the tensile test specimens were machined from the test bars. The tensile test was performed at room temperature, T = 20°C, and at an elevated temperature, T = 480°C, which reflects the approximate temperature range in a continuous galvanizing bath. The results of the tests at T = 20°C can be seen in Fig. 2 and the results of the tests at T = 480°C are summarized in Fig. 3.

The mechanical properties of the martensitic-ferritic alloys at T = 20°C are twice as high as the mechanical properties from the ferrite-free 1.4409.01 material with respect to their mechanical strength. The yield strength of the martensitic-ferritic alloys is in a range of 500 MPa to 900 MPa, and the 1.4409.0 ferrite-free material is below 300 MPa. The elongation at fracture is for the 1.4095 and for the 2.5%Si–4%Cr and 2%Si–4%Cr in the range of 15% to 20%. The 1.4096 and the 3%Si-containing martensitic-ferritic alloy is around 0%. The austenitic 1.4409.01 material has an elongation at fracture around 50%. When it comes to the mechanical properties of the observed samples (Fig. 3) at T = 480°C, some differences can be seen. The mechanical property of the martensitic-ferritic alloy is decreased with respect to yield strength and ultimate tensile strength. The decrease in numbers is around 150 MPa; only the 1.4096 material shows almost no reduction. The ferrite-free austenite 1.4409.1 has decreased the yield strength more than 50%. At the test temperature of T = 480°C, all martensite shows elongation at fracture around 10% to 20%. Remarkable is the increase in the elongation at fracture for the 1.4096 and the 3%Si-containing martensitic-ferritic alloy. The ferrite-free 1.4409.01 keeps its elongation at fracture around 50% at T = 480°C.

Figure 3

Summary of the results of the tensile tests of the tested martensitic-ferritic and austenitic alloys. On the left side the yield strength and the ultimate tensile strength is shown (all values in MPa/N/mm^2), while on the right side the elongation at fracture is presented in %. The test temperature was for this series T = 480°C.

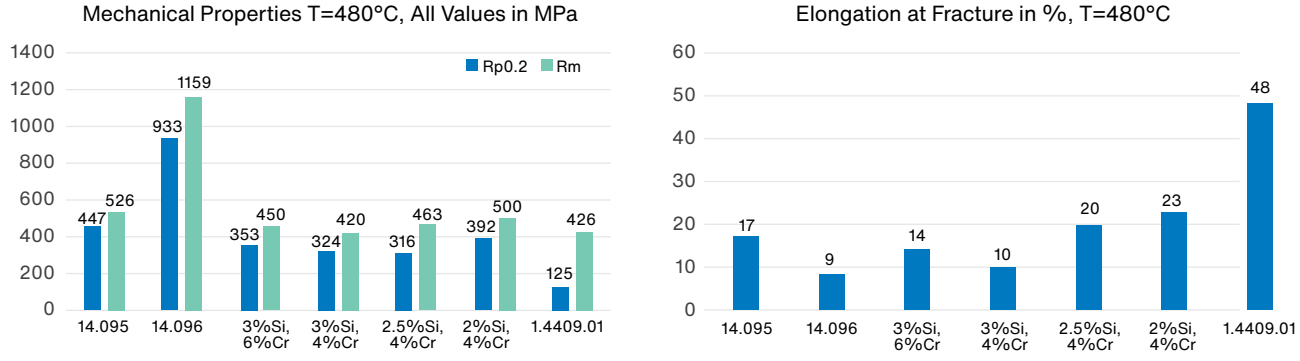

Figure 4

Macroscopic results of the corrosion test at T = 480°C for 715 hours is presented. All samples have a massive Zn layer around each sample on the upper part of the sample. The lowest parts of the sample are already cut off the samples for the microscopy.

Macroscopic Results and Corrosion Tests

After 715 hours in the Zn bath at a temperature of T = 480°C, the samples were removed out of the test rig and in the first step compared macroscopically. The macroscopic picture of these samples can be found in Fig. 4. On the left side, the 1.4095, 1.4096 and the ferrite-free 1.4409.01 material can be seen. On the right side, the different samples with the variation of the Cr and Si content are presented. The samples on the right side were brittle so that some samples were torn up during removal from the test rig.

After the test at 500°C, it was visible that a huge amount of buildup of Zn originated on the sample holder after several hours only (see Fig. 5 right side as a reference). The amount of built-up Zn increased continuously, so that the experiment was canceled after 100 hours (the plan was also a test duration of around 700 hours). During removal, the sample holder broke and some samples were lost. The samples caught were afterwards analyzed via OES so that the traceability was ensured.

A huge amount of built-up Zn can be found on the sample holder. During the removal of the sample holder from the test rig, the complete sample holder was broken, and the samples were caught out of the bath (if possible). The individual samples were then identified via OES since there was no traceability possible anymore. On the right side of Fig. 5, the remains of the sample holder and some caught samples are presented.

The samples that survived the test at T = 500°C for 100 hours are presented in Fig. 6. The 1.4096 and 2.5%Si-4%Cr sample exhibit large Zn layer buildups. This can be an artifact from the removal of the samples out of the Zn pot. There is already a small piece cut off for the OES analysis and the microsection.

All samples have a Zn layer around each sample on the upper part of the sample. The lowest parts of the sample are already cut off the samples for the microscopy. Only four from the seven samples could be caught after the breakdown of the test rig.

The other three tested samples were lost during the extraction of the sample holder after the test.

Figure 5

The left side shows the test rig in the furnace prior to the end of the test at T = 500°C after a duration of 100 hours, and the right side shows the buildup of Zn on the sample holder after several hours.

Figure 6

Macroscopic results of the corrosion test at T = 500°C for 100 hours.

Table 4

The Diameter of the Cross-Section of the Tested Samples After the Corrosion Test at T = 480°C and 715 hours and T = 500°C and 100 hours. There are only little changes in the diameter of the samples.

Material	Initial Ø	Ø after 715 hours at 480°C	Ø after 100 hours at 500°C
1.4409.01	10.02	9.99	10.01
1.4095	10.03	9.98	lost
1.4096	10.01	9.97	9.81
3%Si, 6%Cr	10.03	10.01	lost
3%Si, 4%Cr	10.01	9.99	9.91
2.5%Si, 4%Cr	10.02	9.65	9.75
2%Si, 4%Cr	10.03	9.97	lost

A fast and reasonable way to get information about the corrosion behavior of the tested alloys is to measure the diameter of the samples prior to and after the test. The measurement is done by measuring the outer diameter of the cross-section of the sample after the corrosion test.[4]

The initial diameter of all tested samples is in the range of 10.01 mm to 10.03 mm. After the static corrosion test in the liquid Zn bath for 715 hours at T = 480°C, the diameter of the samples changes slightly. All samples tested, except for the 2.5%Si-4%Cr sample, retained approximately the same diameter after the test. The diameter of the 2.5%Si-4%Cr is reduced to 9.65 mm after the corrosion test. If the test temperature is increased to T = 500°C and the corrosion test time is 100 hours, the diameters of the surviving samples are at the same level as in the initial state — except for the 2.5%Si-4%Cr sample. The diameter of the 2.5%Si-4%Cr samples decreased to 9.75 mm after this test.

Optical Microscopy, SEM and X-Ray Diffraction Results

In this part, the results from the optical microscopy and SEM are presented. Cross-sections from all tested samples were prepared for the optical microscope and some of them were evaluated by means of SEM and EDX for the 1.4096 material for both corrosion tests. The interface between the liquid Zn bath and the sample is summarized in Fig. 7 for the corrosion test at T = 480°C for 715 hours. The cross-section of the 1.4095 exhibits a narrow corrosion interface with sharp-edged inclusions.

Figure 7

Summary of the optical microscopy from the cross-sections of the tested samples at T = 480°C for 715 hours of corrosion.

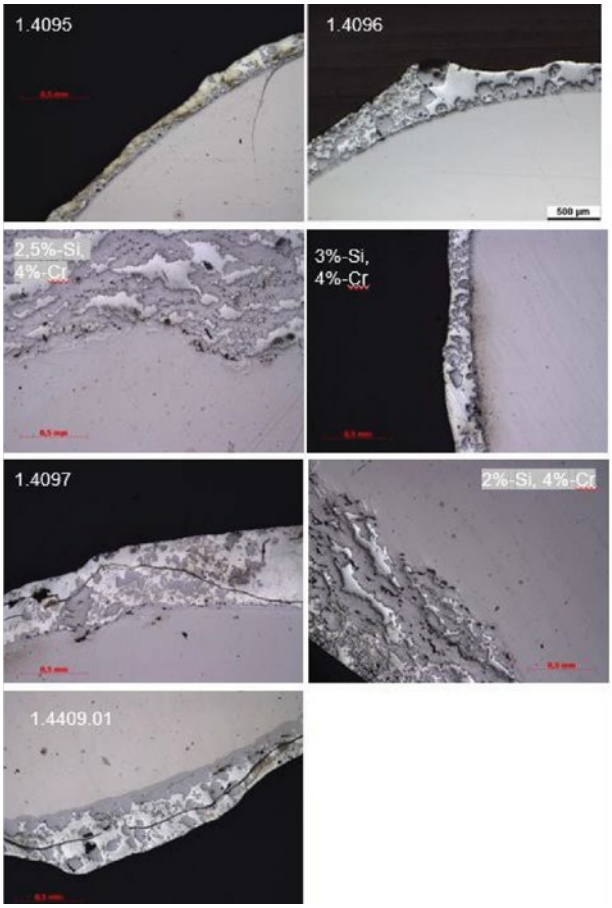

The 1.4096 material also appears with a narrow corrosion interface with inclusions. The next sample is the 2.5%Si-4%Cr sample, which has a thick corrosion layer with a different morphology of inclusions/islands. These inclusions are elongated and larger in comparison to the 1.4095 and 1.4096 material.

All tested samples have a corrosion layer around the base material. The morphology and the amount of different colored regions are different for almost every tested sample. The 1.4095 material shows a relative narrow interface with embedded larger sharp-edged inclusions in the corrosion layer. The 2%Si-4%Cr samples also show a corrosion interface with embedded elongated particles/inclusions. The 1.4409.01 material shows a narrow darker layer without inclusions followed by a thicker layer with inclusions.

The corrosion boundary of the 3%Si-4%Cr sample in Fig. 7 exhibits a slim corrosion layer with small, more angular precipitations. This corrosion layer looks like the corrosion layer of the 1.4096 material. The next cross-section presents the result of the corrosion test

Figure 8

Summary of the optical microscopy from the surviving samples from the static corrosion test at T = 500°C for 100 hours.

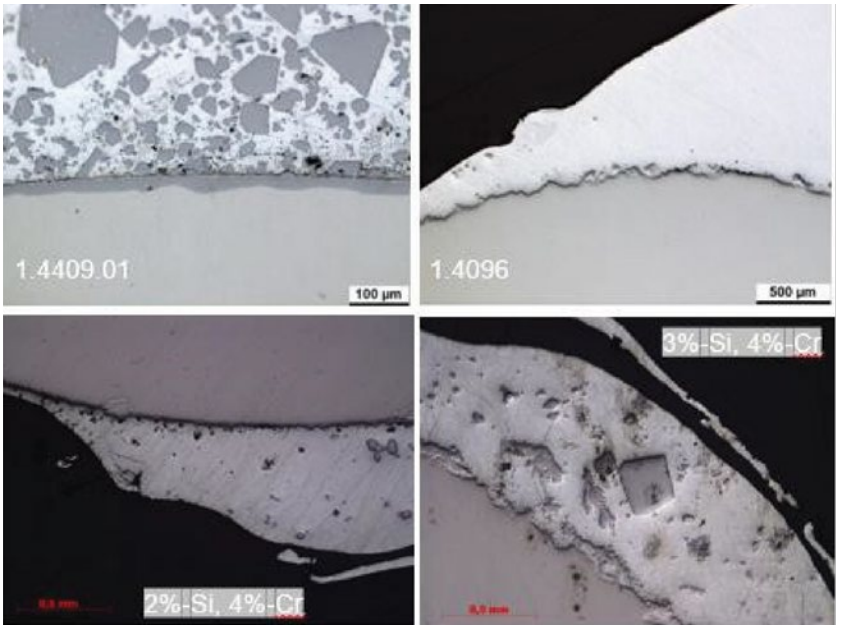

Figure 9

Optical microscopy and scanning electron microscopy (SEM)/energy-dispersive x-ray spectroscopy (EDX) results from the corrosion test at T = 480°C for 715 hours are shown for the 1.4096. (a) and (b) present results from the optical microscopy.

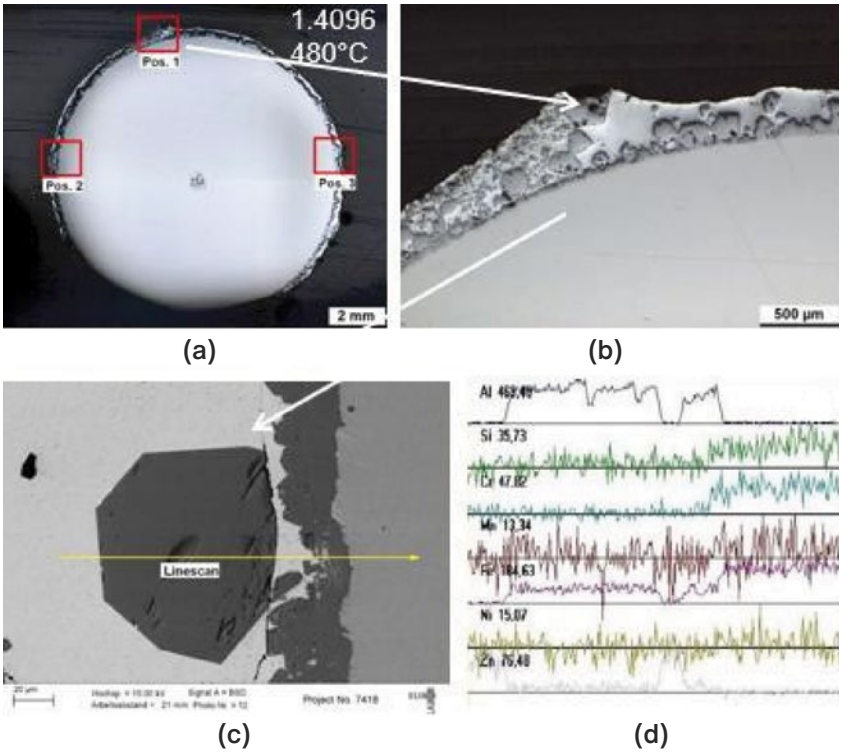

of the 1.4097 sample. The 1.4097 sample has a corrosion interface with blocky smaller and larger inclusions. In contrast to this, the 2%Si-4%Cr sample has elongated precipitates in the interface. The last cross-section from Fig. 7 presents the cross-section from the ferrite-free 1.4409.01 material. A corrosion layer with embedded precipitates in the layer can be seen.

The 1.4409.01 material shows a narrow darker layer without inclusions followed by a thick layer with inclusions and blocky precipitates. The corrosion layer of the 1.4096 materials shows almost no inclusions after the test at 500°C. The samples with 2%Si-4%Cr and 3%Si-4%Cr show interfaces with some precipitates. The sample with the increased Si content shows a larger amount of the precipitates in these micrographs.

The interface between the liquid Zn bath and the sample is summarized in Fig. 8 for the corrosion test at T = 500°C for 100 hours. The 1.4409.01 material presents a thin layer at the interface of the 1.4409.01 material followed by a thick layer with larger and smaller precipitates. In contrast to this, the 1.4096 material presents an almost inclusion-free corrosion layer. The last two pictures from the 2%Si–4%Cr and 3%Si–4%Cr show layers with some inclusions. It seems that the sample with the higher Si content contains more inclusions.

Fig. 9 and Fig. 10 present the SEM and EDX line scan result from the 1.4096 material after the static corrosion test at T=480°C, 715 hours (Fig. 9) and the test at T = 500°C for 100 hours (Fig. 10). The structure of the images is identical for both experiments. Images (a) and (b) reveal the light microscope images of the sample for an overview (a) and an enlarged area (b). Image (c) is a magnified SEM image of (b). The arrow in image (c) marks the course of the EDX spectra in (d). The quantitative analyses of the elements Al, Si, Cr, Mn, Fe, Ni and Zn are presented one below the other. The line scan in Fig. 9 shows, e.g., for the element Al, no signal at the starting point. When the analysis arrives the

dark blocky inclusion in (c), a strong increase in the Al signal is present. Between the particle and the layer around the sample, the Al signal drops back to zero. In the base material, the signal for Al is at zero. For the element Zn in (d) in Fig. 9, an opposite effect of the Zn line scan signal is obvious. The signal starts with a high-level signal and drops down to almost zero when the dark blocky particle is analyzed. Between both darker regions, the Zn signal goes up again. The course of the Fe analysis line corresponds to that of the Al analysis line with the difference that the Fe line is high in the base material. A detailed analysis of the EDX result of the corrosion test at T = 500°C and 100-hour duration (Fig. 10) shows the darker precipitate and the darker thin layer have the same tendency with respect to the signals of Al, Zn and Fe. The sample has a corrosion layer with a Zn-rich chemical analysis. In this layer, particles/precipitates are embedded with an increased Al and Fe content. Most likely the analyzed samples of the 1.4096 material have an Al and Fe-rich thin layer around the sample for both test parameters used in this study.

Figure 10

Optical microscopy and SEM/EDX results from the corrosion test at T = 500°C for 100 hours are shown for the 1.4096. (a) and (b) present results from the optical microscopy.

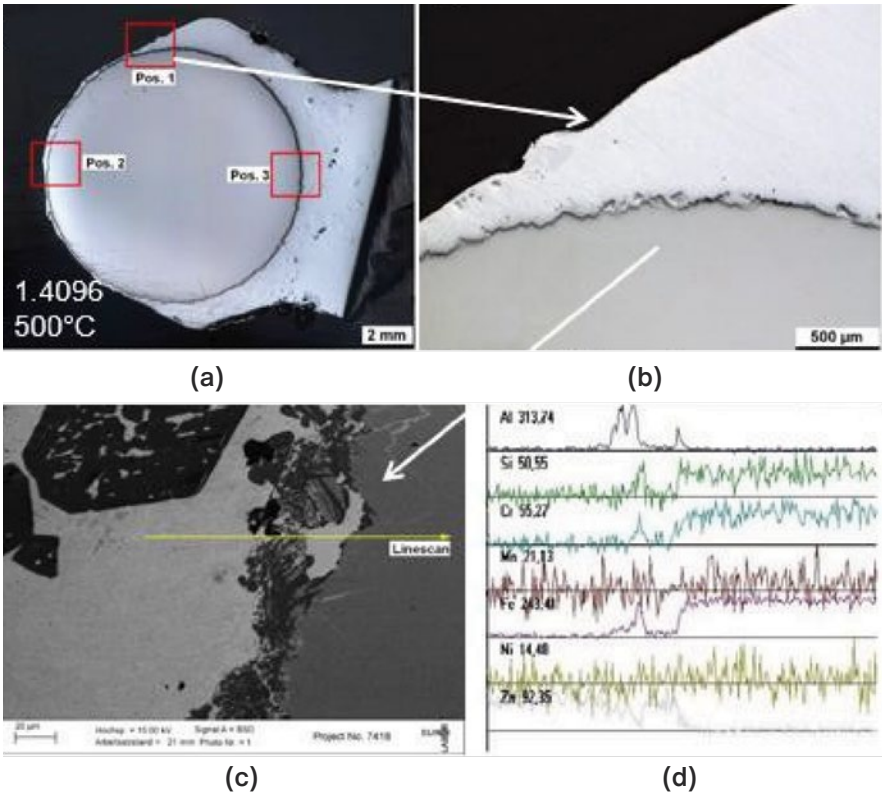

The Pos. 1 in (a) is the enlarged position I (b). (c) shows a detail of (b) at a higher magnification in the SEM. The arrow in (c) refers to the EDX line scan in (d) for different chemical elements. The elements Al, Si, Cr, Mn, Fe, Ni and Zn were analyzed.

Discussion

In this study, different martensitic-ferritic cast alloys (based on the 1.4095 martensite) and the ferrite-free 1.4409.01 austenite were tested with respect to their mechanical properties and their static corrosion behavior in a liquid Zn bath at different test temperatures and corrosion times. The mechanical properties for the heat-treated 1.4095, 2.5%Si-4%Cr and 2%Si-4%Cr are almost double as high as the austenite with respect to mechanical strength; meanwhile the elongation at fracture has values above 10% (Fig. 2). The 1.4096 and the alloys with 3%Si come into view with high mechanical properties with almost no elongation at fracture with this heat treatment. When the test temperature is increased to T = 480°C for the tensile test, the mechanical strength of all samples decreased — meanwhile the elongation at fracture increases or stays at the same level (Fig. 3). The yield strength for all tested martensitic-ferritic alloys is at least twice as high as the ferrite-free austenitic 1.4409.01. How the mechanical properties of the samples are possibly changed during long-term service at elevated temperature has not been examined in this study. In this study, two static corrosion test series were performed: The first one at T = 480°C for 715 hours and the second one at T = 500°C for only 100 hours because the test rig failed. Only four samples could be analyzed from this test. The reason for the failure of the test rig has not been clarified. Most likely the built-up Zn-layer also corroded the sample holder so that it failed. No sample was dissolved during the corrosion tests. Only one sample was attacked by the liquid Zn bath so that a reduction in diameter was measured (see Table 1). The 2.5%Si-4% Cr showed a reduction in diameter of about 0.3 mm after both corrosion tests. In previous tests, the corrosion samples in 1.4095 and 1.4096 dissolved completely (T = 490°C and T = 495°C, test time t = 200 hours).[5] In this study, no sample was dissolved completely in the Zn bath, even not at the test temperature of T = 500°C. The test duration

was only 100 hours and in the Zn bath Al content was added in contrast to the former study.[5] All tested alloys exhibited a surrounding corrosive layer almost always with embedded inclusions (Fig. 7 and Fig. 8). The optical microscopy presents for all samples an intermetallic layer with a brighter and a darker phase like already found in former experiments.[6,7] These intermetallic layers were analyzed in detail with SEM and EDX line scans for the 1.4096 material after both corrosion tests (Fig. 9 and Fig. 10). In Fig. 9c and 9d, the brighter phase consists of a Zn-based composition. The larger inclusion is an Al-Fe-rich particle. Most likely there is an Al_x-Fe_y-phase.[4] The same results with respect to the EDX result from the 1.4096 corrosion test at T = 500°C and t = 100 hours can be seen in Fig. 10c and 10d. Maybe different types of Al_x-Fe_y precipitates are present. This needs to be clarified via different analyzing methods like x-ray phase analysis.

Summary

The present study conducted static corrosion tests in a liquid Zn bath at temperatures of T = 480°C for 715 hours and T = 500°C for 100 hours on seven different materials. The aim was to evaluate the macroscopic and microscopic behavior of the tested alloys, including their mechanical properties at T = 20°C and T = 480°C. The results are presented by showing the reduction in diameter after the experiments. All tested materials survived both test series with almost no reduction in diameter. Both test series underwent optical microscopy and SEM/EDX analysis to evaluate their corrosion resistance. Not all samples were evaluated due to a test rig failure during the T = 500°C experiment. The test rig will be reconstructed and the T = 500°C test will be repeated in the next step.

This article is available online at AIST.org for 30 days following publication.

References

1. "Zinc/Zinc-Alloy/Aluminum Continuous Sheet Coating Lines," Galv Info Center, International Zinc Association, North America, 2022.
2. H. O'Cleary, "Zinc's Price Down, But Not Out," *International Zinc Conference (Europe),* 2022, Istanbul, Turkey.
3. M. van Leeuwen, "Current Status and Future Expectations for the Zinc Market," *InterZAC 2022,* Jackson, Miss., USA, 2022.
4. T. Simon et al., "Corrosion Behaviour of Different Alloys in Zn&Al-Alloys," Galvanizers Association Meeting, Charleston, S.C., USA, 2019.
5. T. Simon et al., "Effect of Zn Bath Temperature on the Corrosion Behavior of Martensitic Steels 1.4095, 1.4096 and 1.4097 in Comparison to the Ferrite-Free Austenitic Steel 316L," *Iron & Steel Technology,* Vol. 21, No. 3, 2024, pp. 90–96.
6. X. Liu et al., "Liquid Metal Corrosion of 316L, Fe3Al, and FeCrSi in Molten Zn-Al Baths," *Metallurgical and Materials Transactions A,* Vol. 36, Issue 8, 2005, pp. 2049–2058.
7. W.J. Wang et al., "The Corrosion of Intermetallic Alloys in Liquid Zinc," *Journal of Alloys and Compounds,* Vol. 428, 2007, pp. 237–243.

AISTech This paper was presented at AISTech 2024 — The Iron & Steel Technology Conference and Exposition, Columbus, Ohio, USA, and published in the AISTech 2024 Conference Proceedings.

Did You Know?

Maruichi Leavitt Pipe & Tube Partners With Chaberton Energy to Install Solar at Chicago Campus

Maruichi Leavitt Pipe & Tube (MLP&T), an industry-leading steel tubing manufacturer, has taken a significant step toward its sustainability and cost-containment goals by partnering with Chaberton Energy to install a solar power generation plant at its 44-acre corporate campus in Chicago.

The multiphased project uses a hybrid approach to address on-site energy needs for the company as well as provide clean energy access to the community through a subscription-based community solar program. Once complete, the project will be one of the largest solar installations in the City of Chicago, spanning more than 1 million square feet, or 24 acres, of MLP&T's campus.

Across its decades-long lifespan, the project is expected to reduce carbon emissions by more than 282,000 metric tons, equivalent to the amount of carbon sequestered by planting 4.7 million trees.

"This solar installation represents a critical milestone in our sustainability goals," said Shunsaku Honda, president of Maruichi Leavitt Pipe & Tube. "The solar array will reduce our carbon footprint and control electric costs while demonstrating our commitment to supporting local community energy needs."

This project marks MLP&T's first U.S. solar installation. The company is part of the Maruichi Steel Tube Group, a global manufacturing organization headquartered in Japan. Chaberton helps customers like MLP&T control energy costs and decarbonize their operations. The manufacturing sector is particularly well-suited for these initiatives, as companies can offset their typically high energy consumption while becoming more self-sufficient.